

Bose-Einstein Condensation of ^{88}Sr Through Sympathetic Cooling with ^{87}Sr

P. G. Mickelson, Y. N. Martinez de Escobar, M. Yan, B. J. DeSalvo, and T. C. Killian
Rice University, Department of Physics and Astronomy, Houston, Texas, 77251
 (Dated: September 15, 2018)

We report Bose-Einstein condensation of ^{88}Sr , which has a small, negative s -wave scattering length ($a_{88} = -2a_0$). We overcome the poor evaporative cooling characteristics of this isotope by sympathetic cooling with ^{87}Sr atoms. ^{87}Sr is effective in this role in spite of the fact that it is a fermion because of the large ground state degeneracy arising from a nuclear spin of $I = 9/2$, which reduces the impact of Pauli blocking of collisions. We observe a limited number of atoms in the condensate ($N_{max} \approx 10^4$) that is consistent with the value of a_{88} and the optical dipole trap parameters.

Bose-Einstein condensation of ^{88}Sr has been pursued for over a decade because of the promise of efficient laser-cooling to high phase space density using the $(5s^2)^1S_0$ - $(5s5p)^3P_1$ narrow intercombination line [1] and loading of optical dipole traps that operate at the magic wavelength for this transition [2]. Recent interest in ^{88}Sr has focused on long-coherence time interferometers [3], optical frequency standards [4, 5], and the existence of low-loss optical Feshbach resonances [6, 7]. There has also been great interest generally in quantum degenerate gases of alkaline-earth metal atoms and atoms with similar electronic structure because of potential applications in quantum computing in optical lattices [8–10] and creation of novel quantum fluids [11].

Early attempts to evaporatively cool ^{88}Sr to quantum degeneracy in an optical dipole trap [2, 12] were not successful in spite of initial phase space densities as high as 10^{-1} , presumably because of a small elastic scattering cross section. This was confirmed by measurements of the scattering lengths of all strontium isotopes using photoassociative [13, 14] and Fourier-transform [15] spectroscopy of Sr_2 molecular potentials, which found that $a_{88} = -2a_0$, where $a_0 = 5.29 \times 10^{-11}$ m is the Bohr radius. Here, we report Bose-Einstein condensation (BEC) of ^{88}Sr through sympathetic cooling with ^{87}Sr .

Divalent atoms such as strontium and ytterbium [16, 17] often possess a large number of stable isotopes, which enables mass tuning of the s -wave scattering length. For strontium, the stable isotopes and abundances are ^{88}Sr (82.6%), ^{87}Sr (7.0%), ^{86}Sr (9.9%), and ^{84}Sr (0.6%). In such systems, the likelihood of finding an isotope with a scattering length that enables efficient evaporative cooling is very high, as was recently demonstrated through the condensation of ^{84}Sr ($a_{84} = 123a_0$) [18, 19]. For an isotope that has a poor scattering length for evaporative cooling, there are also numerous opportunities to find another isotope that can be used effectively for sympathetic cooling. For ^{88}Sr , the fermionic isotope ^{87}Sr is well-suited for this role. It has a large and positive s -wave scattering length of $a_{87} = 96a_0$ [14, 15] which leads to efficient thermalization and evaporation as long as the system is not highly polarized. The inter-isotope scattering length is also reasonable, $a_{88-87} = 55a_0$ [14, 15], so that in a

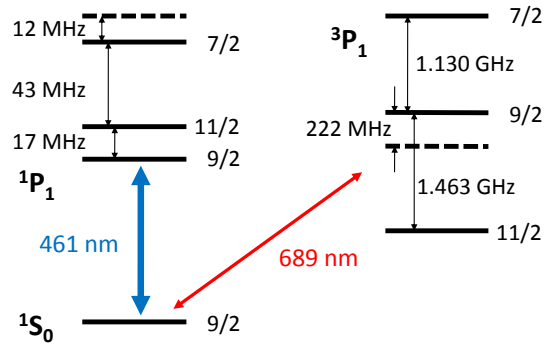


FIG. 1: (color online) Partial level diagram for ^{88}Sr (- -) and ^{87}Sr (—) showing hyperfine structure and isotope shifts [22–24]. Total quantum number F is indicated for ^{87}Sr levels.

mixture, ^{88}Sr will be efficiently cooled (and evaporated) through collisions with ^{87}Sr .

Bosons are normally used to sympathetically cool fermions [20] rather than the other way around, because identical fermions suffer from collisional Pauli blocking, which reduces evaporation efficiency in the quantum degenerate regime [21]. We do not observe significant limitations due to Pauli blocking in the experiments reported here, and we suspect this is because ^{87}Sr has a large nuclear spin ($I = 9/2$) and ground state degeneracy. This suppresses the Fermi temperature and allows ^{88}Sr to be cooled to high phase space density before Pauli blocking of ^{87}Sr collisions becomes important.

Details about our apparatus can be found in refs. [14, 19, 25]. Formation of ultracold mixtures of strontium isotopes benefits from the ability to magnetically trap atoms in the metastable $(5s5p)^3P_2$ state [12, 26–28], which has a 10 min lifetime [29]. One isotope is trapped from a Zeeman slowed beam in a magneto-optical trap (MOT) operating on the $(5s^2)^1S_0$ - $(5s5p)^1P_1$ transition at 461 nm. This transition is not closed and approximately 1 in 10^5 excitations results in an atom decaying through the $(5s4d)^1D_2$ state to the $(5s5p)^3P_2$ state, where it can be trapped in the quadrupole magnetic field of the MOT. After accumulating a desired number of atoms, limited by the loading rate and observed 3P_2 lifetime of about 25 s,

the cooling laser frequency is then switched to cool and accumulate another isotope. In our experiment, we load ^{88}Sr for 3 s and then ^{87}Sr [22] for 30 s, which yields an approximately equal number of atoms of each isotope during evaporative cooling. The laser parameters for trapping ^{88}Sr are given in ref. [26]. For trapping ^{87}Sr [27], the laser is approximately 70 MHz red-detuned from the $^1S_0(F = 9/2) \rightarrow ^1P_1(F = 11/2)$ transition (slightly more than 2Γ , where $\Gamma = 30.5\text{ MHz}$ is the natural linewidth of the transition [30]).

3P_2 atoms are returned to the ground state using 60 ms of 3 W/cm^2 of excitation on the $(5s5p)^3P_2 \rightarrow (5s4d)^3D_2$ transition at $3\text{ }\mu\text{m}$ [25]. The isotope shift ($f_{87} - f_{88} = 110\text{ MHz}$) [25] is small compared to the $\sim 500\text{ MHz}$ width of the repumping efficiency curve [31] for ^{88}Sr and the $\sim 3\text{ GHz}$ width of the hyperfine structure in ^{87}Sr [25]. We tune the $3\text{ }\mu\text{m}$ laser 1.6 GHz blue detuned from the ^{88}Sr resonance, which optimizes the ^{87}Sr repumping while reducing the ^{88}Sr number by 80%. This is a reasonable compromise given that the number of ^{87}Sr atoms is the limiting factor in the experiment. The 461 nm MOT is left on at the optimal ^{87}Sr detuning to maximize the number of captured ^{87}Sr atoms, but this is only ~ 5 natural linewidths red-detuned of the $^{88}\text{Sr } ^1S_0 \rightarrow ^1P_1$ transition [22, 23], so it also serves to aid recapture of this isotope. We typically recapture approximately 1.1×10^7 ^{88}Sr and 3×10^7 ^{87}Sr at temperatures of a few millikelvin.

The 461 nm light is then extinguished and 689 nm light is applied to drive the $(5s^2)^1S_0 \rightarrow (5s5p)^3P_1$ transitions and create intercombination-line MOTs for each isotope. The resonance frequencies in each isotope are well-resolved compared to the 7.4 kHz transition linewidth, so the simultaneous MOTs are compatible with each other. The parameters of the $^1S_0 \rightarrow ^3P_1$ lasers for ^{88}Sr and ^{87}Sr [31] are similar to the conditions in ref. [1] and ref. [32] respectively. As many as 70% of the atoms are initially captured in the intercombination-line MOT. (For experiments with one isotope, the loading phase and intercombination-line lasers for the other isotope are omitted.)

After 400 ms of $^1S_0 \rightarrow ^3P_1$ laser cooling, an optical dipole trap (ODT) consisting of two crossed beams is overlapped for 100 ms with the intercombination-line MOT with modest power (3.9 W) per beam. The ODT is formed by a single beam derived from a 20 W multimode, $1.06\text{ }\mu\text{m}$ fiber laser that is recycled through the chamber to produce a trap with equipotentials that are nearly oblate spheroids, with the tight axis close to vertical. Each beam has a waist of approximately $90\text{ }\mu\text{m}$ in the trapping region.

Immediately after extinction of the 689 nm light, the ODT power is ramped in 30 ms to 7.5 W to obtain a trap depth of $25\text{ }\mu\text{K}$. Typically the atom number, temperature, and peak density at this point for both ^{88}Sr and ^{87}Sr are 3×10^6 , $7\text{ }\mu\text{K}$, and $2.5 \times 10^{13}\text{ cm}^{-3}$. The peak phase space density (PSD) for ^{88}Sr is 10^{-2} .

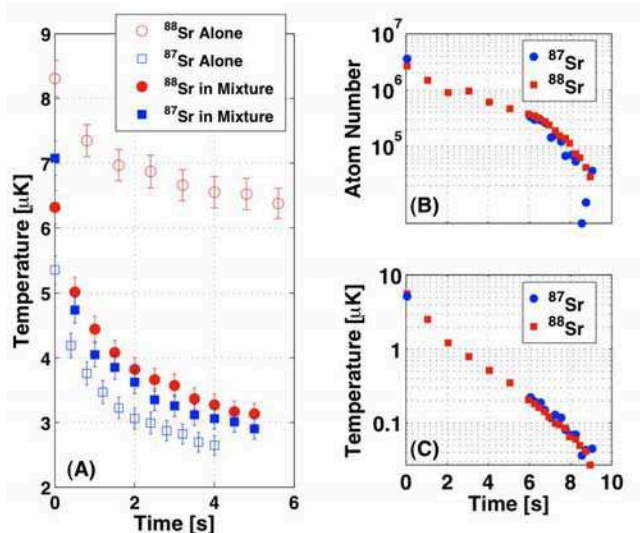


FIG. 2: (color online) (A) Temperature evolution in an ODT with trap depth of $U/k_B = 23\text{ }\mu\text{K}$ for samples of ^{88}Sr and ^{87}Sr alone and for each in a mixture. The number of each isotope present initially is approximately 10^6 . (B) Number and (C) temperature for a mixture along a typical forced evaporation trajectory.

For diagnostics, we record $^1S_0 \rightarrow ^1P_1$ resonant absorption images of samples after a time of flight varying from 10 to 40 ms. Because of broadening of the resonance due to hyperfine structure, ^{87}Sr atoms present would contribute significantly to the absorption when imaging at the ^{88}Sr resonance frequency. To remove ^{87}Sr atoms and obtain clean ^{88}Sr images, light resonant with the $^1S_0(F = 9/2) \rightarrow ^3P_1(F = 11/2)$ transition in ^{87}Sr is applied during the first 2 ms of the time of flight. ^{87}Sr atoms are imaged with linearly polarized light resonant with the $^1S_0(F = 9/2) \rightarrow ^1P_1(F = 11/2)$ transition, and the contamination due to ^{88}Sr is small and easily accounted for [31].

To investigate the collisional properties of the different isotopes and the mixture, the evolution of number and temperature were recorded in a fixed potential (Fig. 2A). For ^{88}Sr alone, evaporation is inefficient and a typical ratio of the trap depth to the sample temperature is $\eta \approx 4$, as observed previously [12]. ^{87}Sr , however, approaches $\eta \approx 9$. Modeling [33] of the free-evaporation trajectory for ^{87}Sr alone suggests a moderate degree of polarization [31] that will be investigated in future studies. The temperatures of ^{87}Sr and ^{88}Sr atoms in a mixture with peak densities of $8 \times 10^{12}\text{ cm}^{-3}$ track each other closely and approach $\eta \approx 8$, indicating that ^{87}Sr provides efficient sympathetic cooling of ^{88}Sr .

Figure 2 shows the number (B) and temperature (C) for a typical forced evaporation trajectory with a mixture. We decrease the laser power according to $P = P_0/(1+t/\tau)^\beta + P_{offset}$, with time denoted by t , $\beta = 1.4$, and $\tau = 1.5\text{ s}$. This trajectory without P_{offset} was designed [34] to yield efficient evaporation when grav-

ity can be neglected. Gravity is a significant effect in this trap for Sr, and to avoid decreasing the potential depth too quickly at the end of the evaporation, we set $P_{offset} = 0.7W$, which corresponds to the power at which gravity causes the trap depth to be close to zero. The lifetime of atoms in the ODT is 30 s. This allows efficient evaporation and an increase of PSD by a factor of 100 for a loss of one order of magnitude in the number of atoms. The ^{87}Sr and ^{88}Sr remain in equilibrium with each other during the evaporation. ^{87}Sr atoms are lost at a slightly faster rate, as expected because essentially every collision involves an ^{87}Sr atom.

Figure 3 shows false color 2-dimensional renderings of (left) and 1-dimensional slices through (right) the time-of-flight absorption images recorded after 16 ms or 22 ms of expansion for various points along the evaporation trajectory. At 5 s of evaporation, the distribution is fit well by a Boltzmann distribution, but at 6 s, a Boltzmann distribution fit to the high velocity wings clearly underestimates the number of atoms at low velocity. A fit using the Bose-Einstein distribution [35], however, matches the distribution well. The fugacity obtained from this fit is 1.0, indicating this is close to the critical temperature for condensation. With further evaporation, the presence of a Bose-Einstein condensate is indicated by the emergence of a narrow peak at low velocity, and eventually, a pure condensate is observed.

At the transition temperature, 2×10^5 ^{87}Sr atoms remain at a temperature of $0.2 \mu\text{K}$. This corresponds to $T/T_F = 0.9$ for an unpolarized sample, which is non-degenerate and above the point at which Pauli blocking significantly impedes evaporation efficiency [21].

^{88}Sr has a negative scattering length, so one expects a collapse of the condensate when the system approaches a critical number of condensed atoms given by [36]

$$N_{cr} = 0.575 \frac{a_{ho}}{|a_{88}|}. \quad (1)$$

Here $a_{ho} = [\hbar/(m\bar{\omega})]^{1/2}$ is the harmonic oscillator length, where m is the atom mass, \hbar is the reduced Planck constant, and $\bar{\omega} = (\omega_x\omega_y\omega_z)^{1/3}$ is the geometric average of the oscillator frequencies. One should also see large fluctuations in the number of condensed atoms during the evaporation due to repeated collapses and refilling of the condensate. To investigate this, we recorded the condensate number for various points in the evaporation trajectory over many experimental runs. For absorption images with a condensate and thermal pedestal, we fit the wings of the thermal cloud, which are beyond the condensate radii of about $23 \mu\text{m}$, to a Bose distribution with fugacity set to 1. The residuals of the fit represent the condensate atoms which are fit with the standard Thomas-Fermi functional form [19, 37] to determine their number.

Figure 4 shows the observed condensate number along the evaporation trajectory from 7 to 10 seconds, as well as maximum values N_{cr} predicted by Eq. 1 where $\bar{\omega}$ is

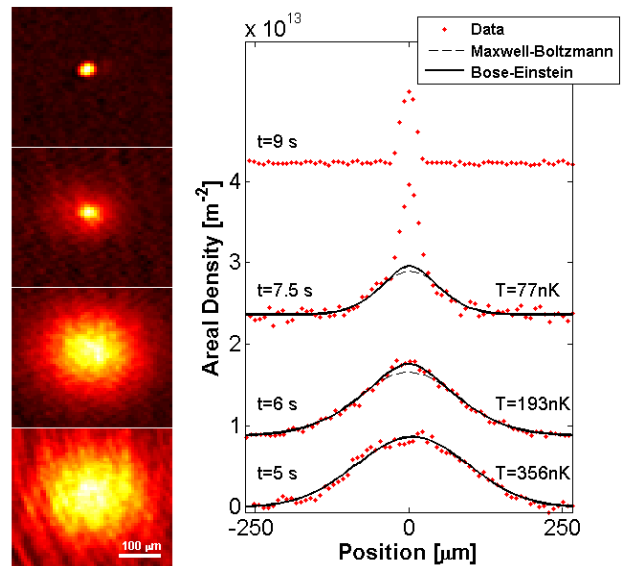


FIG. 3: (color online) Appearance of Bose-Einstein condensation in absorption images (left) and areal density profiles (right). Data correspond to 16 ms (bottom) or 22 ms (top three) of free expansion after indicated evaporation times (t). Images on the left have the same time stamp as on the right. The areal density profiles are from a vertical cut through the center of the atom cloud, and temperatures are extracted from 2D Bose-Einstein distribution fits to the thermal pedestal. At 7.5 s, a bimodal distribution is evident and indicative of Bose-Einstein condensation. For bimodal data, the central region is excluded from the fits and the fugacity is constrained to 1. A pure condensate is shown at 9 s of evaporation.

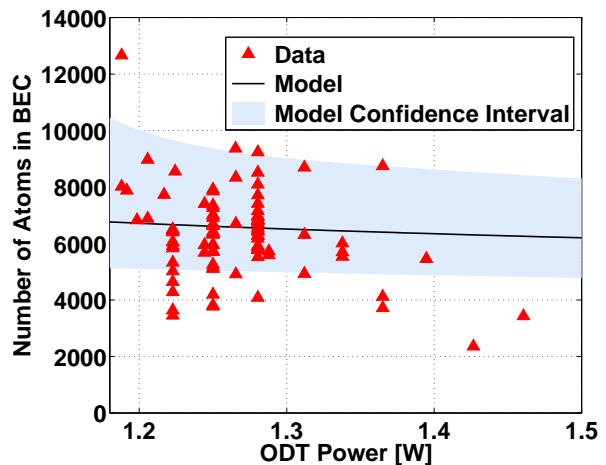


FIG. 4: (color online) Comparison of observed condensate number and maximum condensate number predicted by a model of the trapping potential along the evaporation trajectory.

determined from knowledge of the ODT potential, with confidence intervals reflecting uncertainties of the waists of ODT beams, of about 10%, and the uncertainties of the scattering length $a_{88} = -2.0(3)a_0$ [15]. As expected for attractive interactions, large fluctuations in number are observed. While the best guess curve for N_{cr} falls below some of the data, the upper bound is reasonably well accommodated by the confidence interval. Uncertainties in knowledge of the trap become larger at low ODT power because of the increasingly important role of gravity, which weakens the trap.

We have described the Bose-Einstein condensation of ^{88}Sr through sympathetic cooling with ^{87}Sr . Observation of large fluctuations in number below a maximum number of condensed atoms is consistent with the small, negative value of a_{88} . Because of the very weak interactions, it should be possible to change the sign of the scattering length with an optical Feshbach resonance [6, 7] while keeping induced inelastic losses low. This suggests many possible future experiments, such as creation of matter-wave solitons in two dimensions [38] and quantum fluids with random nonlinear interactions [39].

Acknowledgements This research was supported by the Welch Foundation (C-1579), National Science Foundation (PHY-0855642), and the Keck Foundation.

-
- [1] H. Katori, T. Ido, Y. Isoya, and M. Kuwata-Gonokami, *Phys. Rev. Lett.* **82**, 1116 (1999).
- [2] T. Ido, Y. Isoya, and H. Katori, *Phys. Rev. A* **61**, 061403(R) (2000).
- [3] G. Ferrari, N. Poli, F. Sorrentino, and G. M. Tino, *Phys. Rev. Lett.* **97**, 060402 (2006).
- [4] C. Lisdat, J. S. R. V. Winfred, T. Middelmann, F. Riehle, and U. Sterr, *Phys. Rev. Lett.* **103**, 090801 (2009).
- [5] T. Akatsuka, M. Takamoto, and H. Katori, *Phys. Rev. A* **81**, 023402 (2010).
- [6] R. Ciurylo, E. Tiesinga, and P. S. Julienne, *Phys. Rev. A* **71**, 030701(R) (2005).
- [7] K. Enomoto, K. Kasa, M. Kitagawa, and Y. Takahashi, *Phys. Rev. Lett.* **101**, 203201 (2008).
- [8] A. J. Daley, M. M. Boyd, J. Ye, and P. Zoller, *Phys. Rev. Lett.* **101**, 170504 (2008).
- [9] A. V. Gorshkov, A. M. Rey, A. J. Daley, M. M. Boyd, J. Ye, P. Zoller, and M. D. Lukin, *Phys. Rev. Lett.* **102**, 110503 (2009).
- [10] I. Reichenbach, P. S. Julienne, and I. H. Deutsch, *Phys. Rev. A* **80**, 020701(R) (2009).
- [11] M. Hermele, V. Gurarie, and A. M. Rey, *Phys. Rev. Lett.* **103**, 135301 (2009).
- [12] G. Ferrari, R. E. Drullinger, N. Poli, F. Sorrentino, and G. M. Tino, *Phys. Rev. A* **73**, 023408 (2006).
- [13] P. G. Mickelson, Y. N. Martinez, A. D. Saenz, S. B. Nagel, Y. C. Chen, T. C. Killian, P. Pellegrini, and R. Cote, *Phys. Rev. Lett.* **95**, 223002 (2005).
- [14] Y. N. Martinez de Escobar, P. G. Mickelson, P. Pellegrini, S. B. Nagel, A. Traverso, M. Yan, R. Côté, and T. C. Killian, *Phys. Rev. A* **78**, 062708 (2008).
- [15] A. Stein, H. Knöckel, and E. Tiemann, *Eur. Phys. J. D* **57**, 171 (2010).
- [16] T. Fukuhara, S. Sugawa, Y. Takasu, and Y. Takahashi, *Phys. Rev. A* **79**, 021601(R) (2009).
- [17] T. Fukuhara, Y. Takasu, S. Sugawa, and Y. Takahashi, *J. Low Temp. Phys.* **148**, 441 (2007).
- [18] S. Stellmer, M. K. Tey, B. Huang, R. Grimm, and F. Schreck, *Phys. Rev. Lett.* **103**, 200401 (2009).
- [19] Y. N. Martinez de Escobar, P. G. Mickelson, M. Yan, B. J. DeSalvo, S. B. Nagel, and T. C. Killian, *Phys. Rev. Lett.* **103**, 200402 (2009).
- [20] A. G. Truscott, K. E. Strecker, W. I. McAlexander, G. B. Partridge, and R. G. Hulet, *Science* **291**, 2570 (2001).
- [21] B. DeMarco and D. S. Jin, *Science* **285**, 1703 (1999).
- [22] X. Xu, T. H. Loftus, J. W. Dunn, C. H. Greene, J. L. Hall, A. Gallagher, and J. Ye, *Phys. Rev. Lett.* **90**, 193002 (2003).
- [23] K. Ko, Y. Lim, D. Jeong, H. Park, T. Kim, G. Lim, and H. K. Cha, *J. Opt. Soc. Am. B* **23**, 2465 (2006).
- [24] I. Courtillot, A. Quessada-Vial, A. Bruschi, D. Kolker, G. D. Rovera, and P. Lemonde, *Euro. Phys. J. D.* **33**, 161 (2005).
- [25] P. G. Mickelson, Y. N. Martinez de Escobar, P. Anzel, B. J. DeSalvo, S. B. Nagel, A. J. Traverso, M. Yan, and T. C. Killian, *J. Phys. B* **42**, 235001 (2009).
- [26] S. B. Nagel, C. E. Simien, S. Laha, P. Gupta, V. S. Ashoka, and T. C. Killian, *Phys. Rev. A* **67**, 011401(R) (2003).
- [27] X. Xu, T. H. Loftus, J. L. Hall, A. Gallagher, and J. Ye, *J. Opt. Soc. B* **20**, 968 (2003).
- [28] N. Poli, R. E. Drullinger, G. Ferrari, J. Léonard, F. Sorrentino, and G. M. Tino, *Phys. Rev. A* **71**, 061403(R) (2005).
- [29] M. Yasuda and H. Katori, *Phys. Rev. Lett.* **92**, 153004 (2004).
- [30] S. B. Nagel, P. G. Mickelson, A. D. Saenz, Y. N. Martinez, Y. C. Chen, T. C. Killian, P. Pellegrini, and R. Côté, *Phys. Rev. Lett.* **94**, 083004 (2005).
- [31] P. G. Mickelson, Ph.D. thesis, Rice University (2010).
- [32] T. Mukaiyama, H. Katori, T. Ido, Y. Li, and M. Kuwata-Gonokami, *Phys. Rev. Lett.* **90**, 113002 (2003).
- [33] M. Yan, R. Chakraborty, P. G. Mickelson, Y. N. Martinez de Escobar, and T. C. Killian, arXiv:0905.2223 (2009).
- [34] K. M. O'Hara, M. E. Gehm, S. R. Granade, and J. E. Thomas, *Phys. Rev. A* **64**, 051403(R) (2001).
- [35] W. Ketterle, D. S. Durfee, and D. M. Stamper-Kurn, in *Proc. Int. School of Physics-Enrico Fermi*, edited by M. I. et al. (Amsterdam: IOS Press, 1999), p. 67.
- [36] P. A. Ruprecht, M. J. Holland, K. Burnett, and M. Edwards, *Phys. Rev. A* **51**, 4704 (1995).
- [37] F. Dalfovo, S. Giorgini, L. P. Pitaevskii, and S. Stringari, *Rev. Mod. Phys.* **71**, 463 (1999).
- [38] H. Saito and M. Ueda, *Phys. Rev. Lett.* **90**, 040403 (2003).
- [39] M. P. A. Fisher, P. B. Weichman, G. Grinstein, and D. S. Fisher, *Phys. Rev. B* **40**, 546 (1989).